Stress Distributions in Diblock Copolymers

P. Maniadis, T. Lookman, E. M. Kober, and K. Ø. Rasmussen
Theoretical Division and Center for Nonlinear Studies,
Los Alamos National Laboratory, Los Alamos, New Mexico 87545.
(Dated: March 20, 2007)

We demonstrate how a generalized self-consistent field theory for polymer melts that includes elastic stress and strain fields can be applied to the study of AB diblock copolymers melts. By obtaining the stress distributions for volume conserving strain loadings where lamellar and hexagonal morphologies are stable, we show that the local stress is reduced at the domain interface but slightly enhanced in the immediate vicinity of the interface. The overall stress profile is the result of the combined effects of chain connectivity across the interface, which yields a positive contribution, and the immiscible nature of the monomers, which leads to a stress reduction because of interfacial tension.

Block copolymers spontaneously self-assemble into microphase separated nanodomain structures and the control and optimization of their viscoelastic properties is the key to advances in processing methods [1–4]. In contrast to the mechanical behavior of polymer gels or rubber that form chemically cross-linked networks, block copolymers undergo orientational alignment in the presence of shear which leads to their characteristic property of high tensile strength. The development of methods that incorporate mechanical aspects, in addition to compositional fields, are therefore crucial to exploring the nature of the interplay between deformation and local microstructure. The aim of this work is to demonstrate that self-consistent field methods [5], that have been very successful over the last couple of decades in predicting polymer morphology, can be generalized to yield local equilibrium strains from which bulk elastic properties may be obtained.

The elastic properties of copolymers have been studied by methods that make use of scattering functions [6] or those that monitor changes in the free energy of a given morphology in response to a homogeneous deformation of the unit cell. The free energy is obtained by using a phenomenological model [7] or by the use of a self consistent field approach [8, 9] and a fit to Hooke's law provides an estimate of the elastic moduli. Thus elastic properties of diblock copolymers in the lamelar phase [6, 7], cubic phase [9] and gyroid and body-centered-cubic [8] phases have been studied by such methods which have also been extended to the lamelar phase of multiblock copolymers [10] and ordered nano particle-filled diblock copolymer [11] composites. Although these studies have provided consistent and useful information on the effects of polymer structures on elastic moduli, they do not yield any direct insight into the local stress or strain distributions and how these would vary with different forms of loading. However, Fredrickson [12] has recently proposed a method for homopolymers in which strain fields may be added to the standard self-consistent field theory (SCFT), but the method was not implemented to obtain stress distributions. The aim of this letter is to investigate if strains can be incorporated within SCFT and to demonstrate it on diblock copolymer melts. We calculate the stress distribution that results from an applied volume preserving tensile strain in the regime where the lamellar and hexagonal phases are stable. Moreover, at equilibrium we find that in the interfacial region the stress is reduced as compared to its value in the interior of a domain which is reached by a non-monotonic increase of the stress away from the interface, i.e. there is a region between the interface and the domain center that is characterized by a larger value of the stress. The stress decrease at the interface is a generic property of phase-separating immiscible mixtures, whereas the stress increase arises because the monomers are connected across the interface. We suggest that the resultant stress profile is characteristic of microsegregated materials such as copolymers.

We use a Gaussian microscopic formulation of a polymer solution, expressed in terms of chain conformation variables, that through the use of a Feynman-Kac formula [13] is, converted into a field theory involving four fields. In addition to the two fields [monomer densities, $\phi_{A(B)}$, and their conjugate variables of monomer chemical potentials, $\omega_{A(B)}$] that occur in standard SCFT there is the polymer elastic stress, σ, together with its conjugate field ε, which is the elastic strain. Each polymer chain has degree of polymerization N, and A-monomer fraction f. It is further assumed that each monomer type has the same statistical segment length b. The local interaction between each pair of monomers A and B is quantified by the Flory-Huggins interaction parameter χ. The polymer chains are parameterized by a variable s that increases from 0 to 1 along the length of a chain. A-block starts at $s = 0$ and terminates at the A-B junction point $s = f$. Using this parameterization, it is convenient to define two end-segment distribution functions, $q(r, s)$ and $q^{\dagger}(r, s)$, which are determined by integrating all possible configuration subject to the fields $\omega_A(r)$ and $\omega_B(r)$ for chain segments running from $s = 0$ to f and from $s = f$ to 1, respectively. The distribution function

$q(r,t)$ satisfies the modified diffusion equation

$$\frac{\partial q}{\partial s} = \begin{cases} R_g^2 \nabla\nabla : [\mathbf{m}q] - (\,\omega_A - \mathrm{tr}\,(\varepsilon)\,)\; q & \text{for } 0 \le s < f, \\ R_g^2 \nabla\nabla : [\mathbf{m}q] - (\,\omega_B - \mathrm{tr}\,(\varepsilon)\,)\; q & \text{for } f \le s \le 1, \end{cases} \quad (1)$$

with the initial condition $q(r,0) = 1$. The equation for $q^\dagger(r,t)$ is similar except that the right-hand side of Eq. (1) is multiplied by -1 and the initial condition is $q^\dagger(r,1) = 1$. In Eq. (1) the tensor $\mathbf{m}$ is defined as

$$\mathbf{m}(r;\varepsilon) = \mathbf{1}\,[1 + \mathrm{tr}\,(\varepsilon(r))\,] + 2\varepsilon(r), \quad (2)$$

where $\varepsilon(r)$ and $\mathbf{1}$ are the elastic strain and unity tensors, respectively. The elastic strain tensor is introduced into the theory via its canonically conjugated quantity, the expressions for the microscopic components elastic stress tensor $\sigma(r)$ is [12, 14]:

$$\hat{\sigma}_{jk}(\mathbf{r}) = \frac{2}{4R_g^2}\Big(\sum_{a=1}^{n}\int_0^f ds \frac{dR_{aj}}{ds}\frac{dR_{ak}}{ds}\delta(\mathbf{r}-\mathbf{R}_a) + \sum_{a=1}^{n}\int_f^1 ds\;\frac{dR_{aj}}{ds}\frac{dR_{ak}}{ds}\delta(\mathbf{r}-\mathbf{R}_a)\Big) + \sigma_c\delta(\mathbf{r})\,\delta_{jk} \quad (3)$$

where $\mathbf{R}_a(s) = (R_{ax}(s), R_{ay}(s), R_{az}(s))$ represents the continuous space curve describing polymer chain a. σ_c is a constant isotropic tensor included to ensure that $\hat{\sigma}$ is traceless [15]. At equilibrium the fields $\phi_{A(B)}$ and $\omega_{A(B)}$ must satisfy

$$\omega_{A(B)}(r) = \chi\, N\, \phi_{B(A)}(r) + \xi(r), \quad (4)$$

$$\phi_A(r) + \phi_B(r) = 1. \quad (5)$$

Monomer densities for the A and B species are expressed in terms of the the distribution functions

$$\phi_A(r) = \frac{V}{\mathcal{Z}}\int_0^f ds\, q(r,s)\, q^\dagger(r,s), \quad (6)$$

$$\phi_B(r) = \frac{V}{\mathcal{Z}}\int_f^1 ds\, q(r,s)\, q^\dagger(r,s), \quad (7)$$

where V is the volume of the system and $\mathcal{Z} = \int dr q(r,1)$ the single chain partition function. Similarly can the components of the stress tensor be expressed in terms of the distribution functions

$$\frac{V}{n}\sigma_{jk} = 2N\epsilon_{jk} - R_g^2\delta_{jk}\nabla\nabla:\mathbf{m} - \frac{V}{Z}2R_g^2\delta_{jk}\nabla_l m_{lp}\frac{1}{2}\left\{\int_0^1 ds\; q(\mathbf{r},s)\;\nabla_p q^\dagger(\mathbf{r},s) + \int_0^1 ds\; q^\dagger(\mathbf{r},s)\;\nabla_p q(\mathbf{r},s)\right\} + \frac{V}{Z}2R_g^2 m_{jl}\; m_{kp}\left\{\int_0^1 ds\; q(\mathbf{r},s)\;\nabla_l\nabla_p q^\dagger(\mathbf{r},s) + \int_0^1 ds\; q^\dagger(\mathbf{r},s)\;\nabla_l\nabla_p q(\mathbf{r},s)\right\}. \quad (8)$$

Once the fields and densities are determined to satisfy the self-consistent equations given above the free energy per molecule F is

$$\frac{F}{k_B T} = \chi N\int d\mathbf{r}\;\phi_A\phi_B - \ln\left(\frac{Z}{V}\right) + \frac{1}{V}\int d\mathbf{r}\,[\omega_A\phi_A + \omega_B\phi_B - \varepsilon:\sigma], \quad (9)$$

which reduces to the Flory-Huggins mean-field free energy functional in the unstrained ($\varepsilon = 0$) case. In the general unstrained case we find the periodic morphology that minimizes the free energy in the usual way [16, 17], and then we use Eq. (8) to determine the spatial distribution of the stress tensor. In the case of finite imposed strain the morphology is calculated in a similar manner however the solution of Eq.(1) is now modified. We use the numerical method described in Ref. [16] to calculate the equilibrium configuration of the diblock melt for two different two-dimensional phases a) the hexagonal phase for $f = 0.3$, and b) the lamelar phase for $f = 0.5$.

Initially we solve the self-consistent equations, and calculate the functions q and $q^\dagger$ for zero strain ($\epsilon = 0$). The equilibrium distribution of the A monomers is presented in Fig. 1a for the hexagonal phase, and in Fig. 1d for the lamelar phase. The calculation has been performed on a 64×64 grid, and the minimum of the energy corresponded to a lattice spacing $dx = dy/\sqrt{3} = 0.0725$, for the hexagonal phase, and $dx = dy = 0.07$ for the lamelar phase. Based on the equilibrium configuration, it is possible to determine, using Eq. (8), all the components of the stress tensor σ. The stress components are also given in Fig. 1. Figures 1b and 1e show the σ_{xx} component in the hexagonal phase and in the lamelar phase, respectively, while Figs. 1c, and 1f similarly show the σ_{xy} component. In Fig. 2 we plot the stress profile close to the interface for the lamelar structure of 1a. Even in the absence of external strain we see that the stress distribution is non-uniform. Far from the interface, the stress approaches its zero background value, but it carries a modulation of the background in the vicinity of domain interfaces. These interfaces arise because the incompatibility between A and B blocks makes it energetically favorable for A and B monomers to spatially segregate. However, complete phase separation is impossible because of the covalent

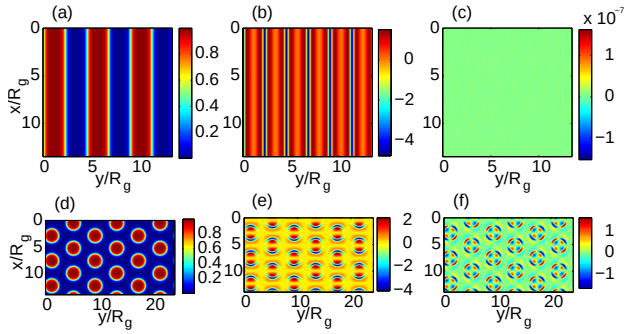

FIG. 1: (Color) Unstrained ($\varepsilon \equiv 0$) equilibrium phases and stress tensor components for $f = 0.3$ (a)-(c) and for $f = 0.5$ (d)-(e). (a) and (d) panels show the A monomer densities. The corresponding tensor components σ_{xx} ((b) and (e)) and σ_{xy} ((c) and (f)) are also shown.

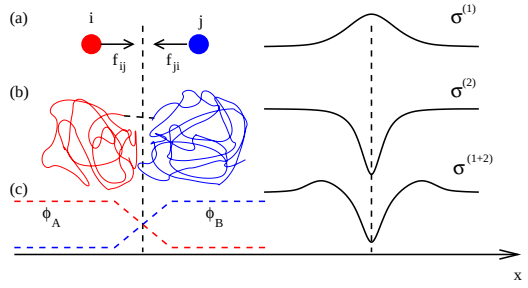

FIG. 3: (Color) Contributions to the total stress profile in the vicinity of an interface (red (blue) color corresponds to A (B) monomers); (a) The stress component $\sigma^{(1)}$ arising from the chain connectivity across the interface (b) The stress component $\sigma^{(2)}$ arising from the immiscibility of the A and B monomers. (c) Shows the density distribution of the A and B monomers and the total stress $\sigma^{(1+2)}$.

bond between A and B blocks, hence domain interfaces are formed. It is, therefore, expected that the middle segments in the interfacial region are predominantly aligned perpendicular to the interface. In accordance with Eq. (3) this alignment also contributes to the value of σ_{ij} in regions where the interfaces are perpendicular to the i or j directions.

We consider the nature of the stress modulation in interfacial regions not perpendicular to either i or j directions. We would expect an increase in the stress at a domain interface because of alignment, and because the chain segments are stretched more than average due to the inherent repulsion of A and B segments in this region. It is, however, apparent from Figs. 1 and 2 that this picture is incomplete. In all cases we observe a *decrease* of the stress at the interface. This stress reduction is always accompanied by a slight increase of stress farther from the interface followed by the final relaxation to the background value. Similar decrease of the mechanical stress has been found using molecular dynamics simulations in [18].

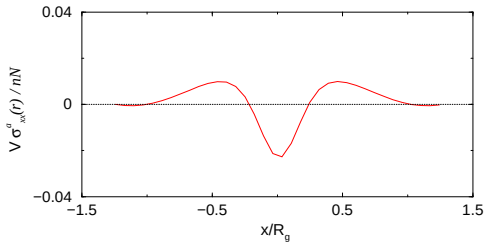

FIG. 2: (Color) Stress (σ_{xx}) profile close to an interface for the lamelar structure shown in Fig.1a.

The separate contributions from distinct parts of the polymer chain allow for an explanation of the stress density profile. Let $\sigma^{(1)}$ be the contribution from the middle segment connecting the A and B blocks, and $\sigma^{(2)}$ the contribution from the remaining segments. On average, the middle segments will be located at the interface and consequently this part of the chain is expected to be stretched resulting in an average attractive force ($f_{ij} = -f_{ji}$ in Fig. 3a) between the A and B monomers across the interface. Because the interface has a width, there is a statistical distribution of these segments in the vicinity of the interface and such bonds contribute to a positive stress density profile as shown by $\sigma^{(1)}$ in Fig. 3a.

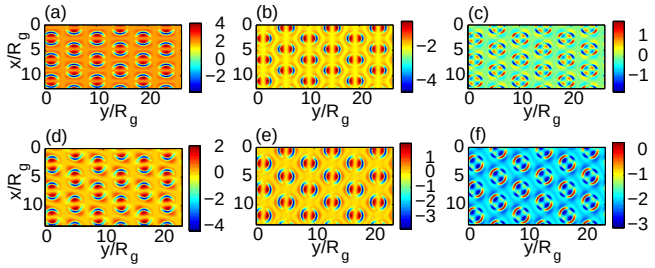

FIG. 4: (Color) Components of the stress tensor for two different nonzero strain applied to the hexagonal phase ($tr\,\epsilon = 0$ for both cases). For $\epsilon_{xx} = -0.1$, $\epsilon_{yy} = 0.1$ and $\epsilon_{ij} = 0$, for $i \neq j$ σ_{xx} (a), σ_{yy} (b), and σ_{xy} (c) are shown. For $\epsilon_{ij} = 0$, for all i, j except $\epsilon_{xy} = -0.1$ the components σ_{xx} (d), σ_{yy} (e), and σ_{xy} (f) are shown.

In contrast, the behavior of $\sigma^{(2)}$ arises from the macroscopic properties of the interface that depend on the form of the densities ϕ_A and ϕ_B [18, 19]. There is an energy cost associated with the creation of the interface, which appears as a positive interfacial tension γ. The interfacial tension can be calculated from the gradient square of the distribution, which will be positive. The iterfacial tension is defined as the difference between the tangential and perpendicular components at the interface and as the tangential component is zero, $\gamma = -\sigma^{(2)}$, giving a negative contribution to the stress $\sigma^{(2)}$ (Fig. 3b). The total stress density is the sum of the individual components, $\sigma^{(1+2)} = \sigma^{(1)} + \sigma^{(2)}$ (Fig. 3c).

The equilibrium stress distribution and energy in the

presence of an applied homogeneous strain ($\epsilon \neq 0$) may be obtained from the modified diffusion equation (1) together with the self consistent equations. Since we limit our investigation to incompressible polymer melts, we must apply a volume preserving strain ($tr\ \epsilon = 0$). In Fig. 4 we present the stress components for the hexagonal phase in the case of a 10% compression strain in the x-direction $\epsilon_{xx} = -0.1$, with $\epsilon_{yy} = 0.1$ in order to preserve the volume (Figs. 4a, 4b, and 4c), as well as in the case of a shear strain with $\epsilon_{xy} = 0.1$ (Figs. 4d, 4e, and 4f). The behavior of the polymer melt in the presence of applied stress is summarized in Fig. (5) where we show the spatially averaged stress as a function of the external strain for the hexagonal phase.

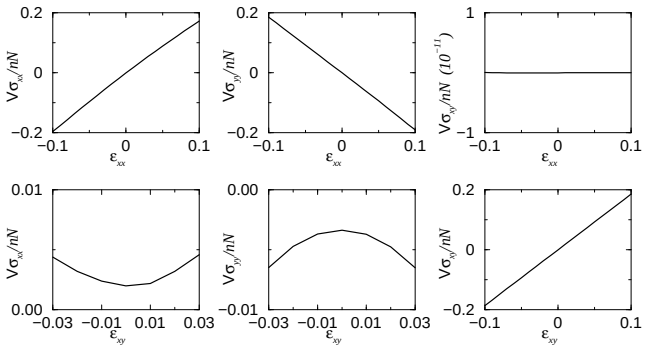

FIG. 5: The spatially averaged components of the stress tensor σ as a function of the external strain ϵ in the hexagonal phase.

In addition to the local effects at the interfaces, the strain also influences the spatially averaged stress distribution. A compression (expansion) of the melt, in the (i, j) directions, leads to a decrease (increase) of the spatially averaged stress in this direction (i,e, a change in σ_{ij}). However, it is also evident from Fig. 5 that σ_{ij} are affected although to a lesser degree. As the applied strain undergoes the relatively large variation from -0.1 to 0.1 we see that the primary stress component changes linearly, whereas the more secondary elements display a nonlinear dependence for larger ($|\epsilon_{ij}| > 0.01$) applied strain.

Figure 5 gives the corresponding components of the elasticity tensor $K_{ij,kl}$ in the linear regime using $\sigma_{ij} = \sum_{kl} K_{ij,kl} \cdot \epsilon_{kl}$. Thompson et al. [10] previously calculated elastic constants by changing the volume and shape of the simulation box. It can be shown that the two methods are equivalent by a simple variable transformation of the coordinates. The present method has the added advantage that it yields insight into the detailed stress distribution over the entire volume of the melt. A method that allows the box shape to also vary under applied stress has recently been proposed [20].

In summary, we have demonstrated how self-consistent field theory may be applied to obtain stress and strain distributions for AB diblock copolymer melts. We have shown that non-trivial stress effects arise at the domain interfaces. Specifically, we have shown that the overall stress increases away from the interface and then decreases to its homogeneous value within the domain. We have also emphasized our methodology's ability to determine morphological and local stress changes resulting from applied strain. Finally, we have shown how linear elastic moduli of a polymer melt in a given morphology may be obtained.

This research was carried out under the auspices of the National Nuclear Security Administration of the U.S. Department of Energy at Los Alamos National Laboratory under Contract No. DE-AC52-06NA25396.

[1] I.W. Hamley, *The Physics of Block Copolymers* (Oxford University Press, Oxford, 1998).
[2] G.H. Fredrickson, F.S. Bates, Annu. Rev. Mater. Sci. **26**, 501 (1996).
[3] G. Holden, N.R. Legge, R. Quirk, H. Schroeder, Eds. *Thermoplastic Elastomers* (Hanser/Gardner Publications, Cincinnati, OH, 1996).
[4] R. G. Larson, *Structure and Rheology of Complex Fluids* (Oxford University Press, New York, 1999).
[5] M.W. Matsen, J. Phys.; Condens. Matter **14**, R21 (2002), and refrences therein.
[6] C. Yeung, A. C. Shi, J. Noolandi, and R.C. Desai, Macromol. Theory Simul. **5**, 291 (1996), and references therein.
[7] Z.G. Wang J. Chem. Phys. **100**, 2298 (2004).
[8] C.A. Tyler and D.C. Morse, Macromolecules **36**, 3764 (2003).
[9] M.B. Kossuth, D.C. Morse and F.S. Bates, J. Rheology **43**, 167 (1999).
[10] R. B. Thompson, K.Ø. Rasmussen, and T. Lookman, J. Chem. Phys. **120**, 3990 (2004).
[11] R. B. Thompson, K.Ø. Rasmussen, and T. Lookman, Nano Letters **4**, 2455 (2004).
[12] G. H. Fredrickson, J. Chem. Phys. **117**, 6810 (2002).
[13] R.P. Feynman and A.R. Hibbs, *Quantum Mechanics and Path Integrals* (McGraw-Hill, New York, 1965).
[14] M. Doi, and S.F. Edwards, *Theory of Polymer Dynamics* (Oxford Universsity Press, New York, 1988).
[15] This constant correspond to the term that was eliminated by Doi end Edwards in the calculation of the stress expresion because it is isotropic. As we have found, this term should be included since its contribution cancels the isotropic part of $\hat{\sigma}$. Calculating the average for a Gaussian chain we find that σ_c is equal to $-\,n\,N/V$.
[16] G. Tzeremes, K. Ø. Rasmussen, T. Lookman and A. Saxena, Phys. Rev. E **65**, 041806 (2002).
[17] F. Drolet and . H. Fredrickson, Phys. Rev. Lett. **83**, 004317 (1999)
[18] Rüdiger Goetz and Reinhard Lipowsky, J. Chem. Phys. **108**, 7397 (1998)
[19] John W. Cahn and John E. Hilliard, J. Chem. Phys. **28**, 258 (1958).
[20] Jean-Louis Barrat, G. H. Fredrickson and Scott W. Sides, J. Phys. Chem. B **109**, 6694-700 (2005).